Transgenic Mice Expressing a Mutant Form of Loricrin Reveal the Molecular Basis of the Skin Diseases, Vohwinkel Syndrome and Progressive Symmetric Erythrokeratoderma

Yasushi Suga,*‡§ Michal Jarnik,‖ Paul S. Attar,* Mary A. Longley,* Donnie Bundman,* Alasdair C. Steven,‖ Peter J. Koch,*‡ and Dennis R. Roop*‡

*Department of Molecular and Cellular Biology and ‡Department of Dermatology, Baylor College of Medicine, Houston, Texas 77030; §Department of Dermatology, Juntendo University School of Medicine, Tokyo 113-8421, Japan; ‖Laboratory of Structural Biology, National Institute of Arthritis and Musculoskeletal and Skin Diseases, National Institutes of Health, Bethesda, Maryland 20892

Abstract. Mutations in the cornified cell envelope protein loricrin have been reported recently in some patients with Vohwinkel syndrome (VS) and progressive symmetric erythrokeratoderma (PSEK). To establish a causative relationship between loricrin mutations and these diseases, we have generated transgenic mice expressing a COOH-terminal truncated form of loricrin that is similar to the protein expressed in VS and PSEK patients. At birth, transgenic mice (ML.VS) exhibited erythrokeratoderma with an epidermal barrier dysfunction. 4 d after birth, high-expressing transgenic animals showed a generalized scaling of the skin, as well as a constricting band encircling the tail and, by day 7, a thickening of the footpads. Histologically, ML.VS transgenic mice also showed retention of nuclei in the stratum corneum, a characteristic feature of VS and PSEK. Immunofluorescence and immunoelectron microscopy showed the mutant loricrin protein in the nucleus and cytoplasm of epidermal keratinocytes, but did not detect the protein in the cornified cell envelope. Transfection experiments indicated that the COOH-terminal domain of the mutant loricrin contains a nuclear localization signal. To determine whether the ML.VS phenotype resulted from dominant-negative interference of the transgene with endogenous loricrin, we mated the ML.VS transgenics with loricrin knockout mice. A severe phenotype was observed in mice that lacked expression of wild-type loricrin. Since loricrin knockout mice are largely asymptomatic (Koch, P.K., P.A. de Viragh, E. Scharer, D. Bundman, M.A. Longley, J. Bickenbach, Y. Kawachi, Y. Suga, Z. Zhou, M. Huber, et al., *J. Cell Biol.* 151:389–400, this issue), this phenotype may be attributed to expression of the mutant form of loricrin. Thus, deposition of the mutant protein in the nucleus appears to interfere with late stages of epidermal differentiation, resulting in a VS-like phenotype.

Key words: loricrin • transgenic • erythrokeratoderma • Vohwinkel's syndrome

Introduction

The formation of the cornified cell envelope (CE)[1] in terminally differentiating keratinocytes is generally accepted to be crucial for the barrier function of the skin (Roop, 1995). The CE represents an insoluble layer of proteins (e.g., involucrin, loricrin, small proline-rich proteins [SPRRs], elafin, cystatin A, S100 family proteins, and some desmosomal proteins) that are covalently cross-linked by ε-(γ-glutamyl)lysine isopeptide bonds formed by epidermal transglutaminases (TGases) (Steven and Steinert, 1994; Steinert and Marekov, 1995).

Loricrin is expressed late in epidermal differentiation and is the major component of the CE, constituting as much as 70% of its mass (Steven and Steinert, 1994). Loricrin is a glycine-, serine-, and cysteine-rich basic protein expressed in the granular cell layer of the epidermis (Mehrel et al., 1990; Hohl et al., 1991), where it is first stored in aggregates (L granules) that are predominantly cytoplas-

Address correspondence to Dennis R. Roop, Department of Molecular and Cellular Biology, Baylor College of Medicine, One Baylor Plaza, Houston, TX 77030. Tel.: (713) 798-4966. Fax: (713) 798-3800. E-mail: roopd@bcm.tmc.edu

M. Jarnik's present address is Fox Chase Cancer Center, Philadelphia, PA 19111.

[1]*Abbreviations used in this paper:* BrdU, bromodeoxyuridine; CE, cornified cell envelope; EGFP, enhanced GFP; GFP, green fluorescent protein; LorNAb, antibody against the NH_2 terminus of loricrin; LorCAb, antibody against the COOH terminus of loricrin; NLS, nuclear localization signal(s); PSEK, progressive symmetric erythrokeratoderma; RPA, RNase protection assay; TEWL, transepidermal water loss; VS, Vohwinkel's syndrome.

mic, but occasionally are seen in the nucleus (Steven et al., 1990; Ishida-Yamamoto et al., 1993). In the last stage of terminal differentiation, these aggregates are dispersed and loricrin is assembled into the CE where it is cross-linked with the other CE components (Steven et al., 1990).

Recently, a mutation in the loricrin gene has been reported in certain subtypes of Vohwinkel syndrome (VS) (Online Mendelian Inheritance in Man [OMIM™] no. 124500, available at http://www.ncbi.nlm.nih.gov/Omim/) (Maestrini et al., 1996; Korge et al., 1997; Armstrong et al., 1998; Takahashi et al., 1999). This was one of the first genetic disorders reported affecting a CE component and the first to be associated with a gene in the epidermal differentiation complex on chromosome 1q21 (Maestrini et al., 1996). Furthermore, Ishida-Yamamoto et al. (1997) identified a similar loricrin mutation in a family with progressive symmetric erythrokeratoderma (PSEK). In the cases reported to date, frameshift mutations in the loricrin gene (due to a single base pair insertion at codon 231 [231insG] or codon 209 [209insT] in VS, or at codon 224 [224insC] in PSEK) have produced mutant forms of loricrin with altered and extended COOH termini, in consequence of alternative, downstream termination signals. Thus, the common feature of all VS-related loricrin mutations described to date is replacement of the COOH-terminal Gly- and Gln/Lys-rich domain with highly charged Arg- and Leu-rich amino acid sequences.

VS is characterized by a diffuse thickening of the epidermis of palms and soles (palmoplantar hyperkeratosis) with small "honeycomb" depressions and progressive formation of constrictions on digits and toes (pseudoainhum) (Vohwinkel, 1929; Gibbs and Frank, 1996). Irregularly shaped thickening of the skin (keratosis) is also seen on the backs of hands and feet, on the knees, and on the elbows. Some VS families also exhibit deafness, whereas others have normal hearing but develop a diffuse congenital ichthyosis (Camisa and Rossana, 1984). On the basis of recent molecular studies, it is now clear that VS associated with deafness is genetically distinct and caused by mutations in connexin 26 (Maestrini et al., 1999), whereas VS associated with ichthyosis is caused by mutations in loricrin (Maestrini et al., 1996; Korge et al., 1997; Armstrong et al., 1998; Takahashi et al., 1999). The PSEK family examined by Ishida-Yamamoto et al. (1997) exhibited widespread erythematous keratotic plaques and palmoplantar hyperkeratosis with pseudoainhum. The clinical differences between VS associated with ichthyosis and PSEK were thought to be due to the insertion site of the mutation. However, it remains to be seen whether the site of mutation will consistently correlate with the respective disease phenotype.

Here, we introduced a transgene into the germline of mice that mimics the loricrin mutations identified previously in VS patients. Transgenic mice expressing this mutant form of loricrin exhibited an erythematous skin phenotype at birth, with a thickening of the epidermis (erythrokeratoderma). Mice expressing the highest levels of the transgene also showed a pseudoainhum-like constricting band around their tail and hyperkeratosis of the footpads around day 7. Thus, these animals represent a new model system which will be useful to study the pathogenesis and potential treatments of human loricrin keratoderma.

Materials and Methods

Construction of the ML.VS Transgene and Generation of Transgenic Mice

We engineered a single nucleotide insertion (C) at position 1190 (codon 372) of the mouse loricrin coding sequence (numbering is according to Mehrel et al., 1990; sequence data available from EMBL/GenBank/DDBJ under accession no. M34398) using PCR-mediated mutagenesis to mimic the mutation found in the families with VS. This point mutation resulted in the generation of an additional Acc65I restriction enzyme site in codon 371 and 372 (position 1186–1191).

A BamHI–PstI fragment of the mouse loricrin genomic DNA (DiSepio et al., 1995) spanning positions 779–1684 was cloned into the pGem3zf(+) vector (Promega) and used as a PCR template. Overlapping PCR products, including positions 779–1203 and positions 1181–1684, were amplified using T7 and Sp6 primers as well as the loricrin-specific primers, oligonucleotide 1 (5′-CCACCTCCACAGGGTACCACCTCC-3′) and oligonucleotide 2 (5′-GGAGGTGGTACCCTGTGGAGGTGG-3′), both of which include an additional Acc65I site in the sequence (underlined). The PCR products amplified with primers T7/oligonucleotide 1 and oligonucleotide 2/Sp6 were subcloned into the pGemT vector (Promega) and sequenced. These 5′ and 3′ mutant DNA fragments were then combined using the Acc65I restriction enzyme site, resulting in a mutated loricrin construct with a C insertion at nucleotide position 1190 (pGemT1190insC). A BamHI–Bsu36I fragment from pGemT1190insC containing the point mutation was then inserted into the 6.5-kb genomic loricrin fragment, replacing the corresponding wild-type sequence. This construct (ML.VS, see Fig. 1) was injected into ICR mouse embryos to produce transgenic mice expressing the mutant loricrin (DiSepio et al., 1995).

Transgenic mice were identified by PCR using tail DNA as a template with oligonucleotide 3 (3′-TCCTCTCAGCAGACCAGTCAGACCT-5′) and oligonucleotide 4 (3′-CTCTTCCAGCTCTGTTGTCTCCGTT-5′), which gave after Acc65I restriction enzyme digestion, a 440-bp band in nontransgenic pups, but 440- and 385-bp bands in transgenics. PCR was performed with 200 ng of genomic DNA using an initial denaturation at 94°C (5 min); followed by 25 cycles with denaturation at 94°C (1 min), annealing at 55°C (2 min), and elongation at 72°C (3 min); and, finally, 15 min at 72°C.

Histology and Immunofluorescence Microscopy

All samples were from the back skin of severely affected F2 transgenics and nontransgenic littermates. Tissues were fixed in Carnoy's solution (chloroform/acetic acid/ethanol, 3:1:6 [vol/vol/vol]) at 4°C overnight, transferred to 95% ethanol, embedded in paraffin, sectioned, and stained with hematoxylin and eosin. Biopsy samples were frozen in OCT (Tissue-TekII; Lab-Tek Products) at −70°C, sectioned at 4–6 μm, and mounted onto glass slides. For immunofluorescence microscopy, the following antibodies were used: guinea pig antibodies to the COOH terminus of loricrin (LorCAb), which were produced against the synthetic peptide CHQTQQKQAPTWPCK (Mehrel et al., 1990); keratin 14 (K14) antibodies (Roop et al., 1984); rabbit antibodies directed to the NH_2 terminus of loricrin (LorNAb), which were produced against the synthetic peptide SHQKKQPTPCPPVGCGKTSG; and antibodies to K6 (Roop et al., 1984). The following secondary antibodies were used: biotinylated goat anti–guinea pig (Vector Laboratories), sheep anti–rabbit conjugated with FITC (Dako), and Streptavidin–Texas red (GIBCO BRL). Double label immunofluorescence was performed as described previously (Roop et al., 1987).

Ultrastructural Analysis

Skin samples were processed essentially as described previously (Jarnik et al., 1996). In brief, back skin biopsies (~1 mm^3) were briefly washed in PBS and fixed for 3 h with three changes in 2% glutaraldehyde in 50 mM cacodylate buffer, pH 7.2, containing 2% sucrose; washed with the same buffer without sucrose; and postfixed two times for 1 h. with 1% osmium tetroxide. After an overnight wash in water, samples were serially dehydrated in ethanol and propylenoxide, infiltrated with EMbed-812 resin (EMS), and polymerized for 24 h at 65°C. Thin sections were stained with 2% uranyl acetate and lead citrate.

For immunocytochemistry, frozen specimens were prepared according to Tokuyasu (1980). The tissue was fixed in 6% formaldehyde in 0.1 M Pipes, pH 7.05; washed with the same buffer; perfused with 2.1 M sucrose; placed on the specimen carrier; and quenched in liquid nitrogen. Thin cryosections were cut, transferred to a drop of 2.3 M sucrose, and mounted on

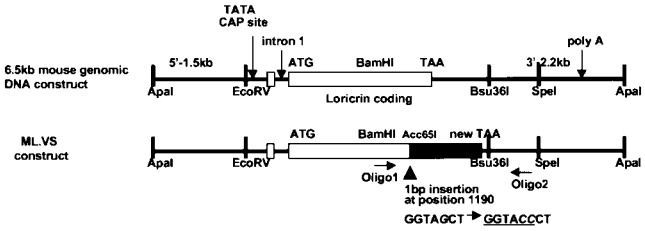

Figure 1. Construction of transgene. Schematic representation of the structures of the ML.VS transgene and the 6.5-kb mouse genomic DNA construct. We introduced a frameshift mutation resulting in a delayed termination of translation (black box) into the second exon (white boxes) of the loricrin gene by inserting a cytosine (C) at position 1190 (arrowhead). An additional Acc65I site was created by the mutation (underlined).

formvar/carbon-coated grids. The immunostaining procedures have been described elsewhere (Steven et al., 1990; Jarnik et al., 1996). The primary antibody for immunocytochemistry was LorNAb, and the secondary label was a protein A–10-nm gold complex (BBInternational).

The specimens were viewed on a ZEISS 902 electron microscope.

Bromodeoxyuridine Labeling Experiments

Age-matched transgenic and normal samples were processed as described previously (Dominey et al., 1993). In brief, newborn transgenic and control mice were injected i.p. with 250 mg/kg body weight bromodeoxyuridine (BrdU) in 0.9% NaCl (Sigma-Aldrich) and killed after 1 h. Dorsal skin was fixed in 70% ethanol at 4°C, embedded in paraffin, and sectioned. Sections were cut, deparaffinized, and soaked in 2 N HCl for 30 min. Sections were rehydrated and dried, and treated with undiluted FITC-conjugated mAb to BrdU (Becton Dickinson) mixed with guinea pig antiserum to mouse K14 for 20 h (Dominey et al., 1993).

Construction of Enhanced Green Fluorescent Protein Vectors and Green Fluorescent Protein Assay in HeLa Cells

A eukaryotic expression vector with an enhanced green fluorescent protein (EGFP) sequence and multicloning sites was used for this assay (pEGFP-C1; CLONTECH Laboratories, Inc.). In brief, various sequences from the COOH terminus of mutant loricrin were fused to the 3′ end of the GFP tag in order to identify potential nuclear localization signal (NLS). 900-bp BamHI–PstI fragments from both the wild-type and the ML.VS mutant loricrin sequence were subcloned into pE6FP-C1 to create GFP(ML BamHI/PstI) and GFP(ML.VS BamHI/PstI) (see Fig. 11). Fur-

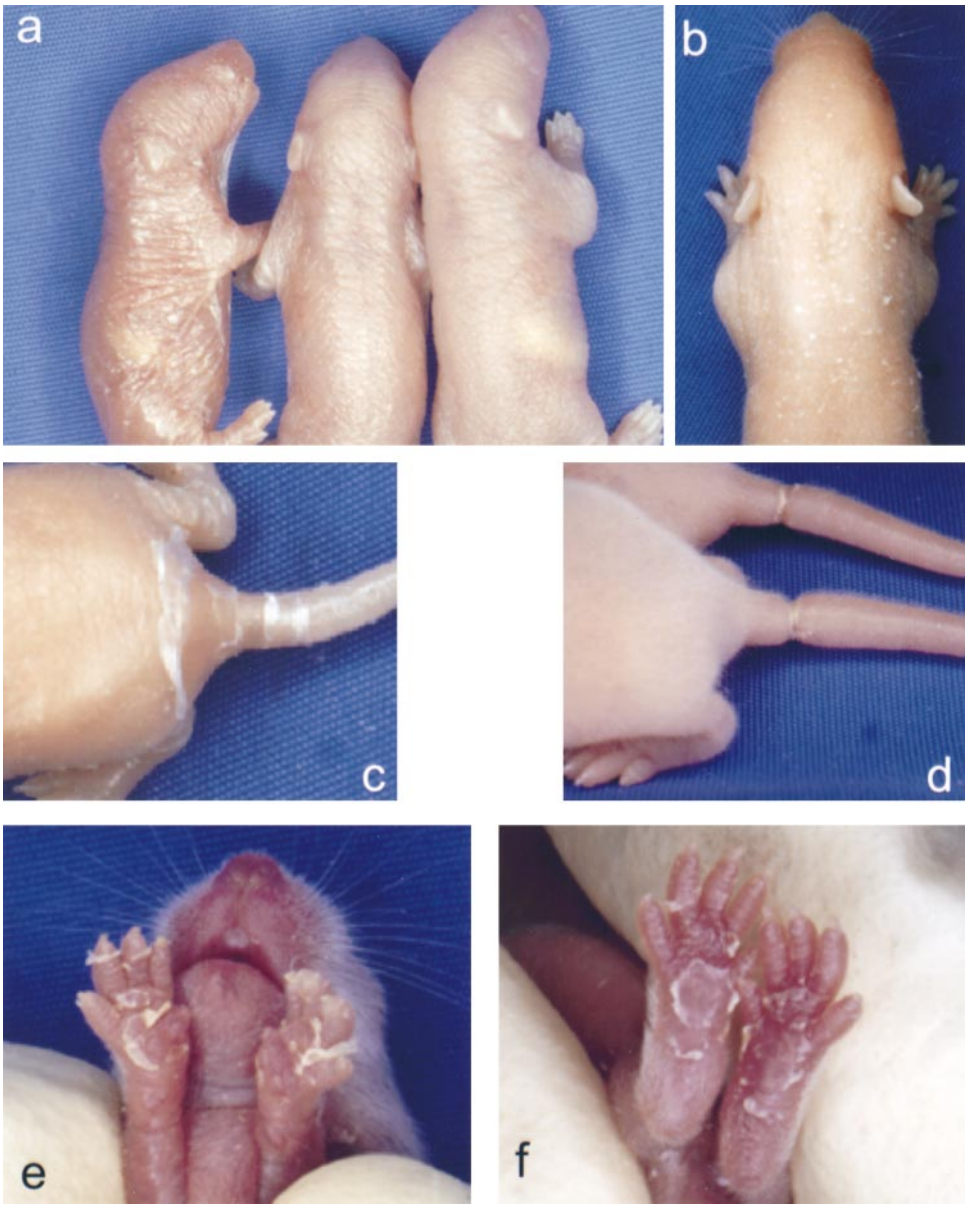

Figure 2. Macroscopic phenotypes of ML.VS transgenic mice. (a) Severely (left) and moderately (middle) affected transgenic neonates, and control (right) littermate F2 pups. Note the erythrokeratoderma with a shiny skin in the transgenic pups. (b) Phenotype of a pup at day 4 after birth. Note the hyperkeratotic, scaly skin, which resembles generalized ichthyosis. (c) Severely affected transgenic mice exhibited hyperkeratotic skin limited to buttocks and tails at day 5 after birth. (d) Hyperkeratotic constricting bands develop at the base of tail at day 7. Note that the distal part of the tail was slightly edematous. (e and f) Front and rear paws of transgenics at day 10. Note the severe scaling of the footpads.

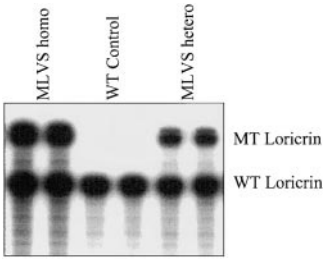

Figure 3. RPAs using RNA from neonatal epidermis. Note the higher expression level of mutant (MT) loricrin transcripts in the severely affected homozygous F2 pups (MLVS homo) compared with the moderately affected heterozygous F2 pups (MLVS hetero). Simultaneous detection of endogenous wild-type (WT) loricrin transcripts provides a loading control.

thermore, a 490-bp Acc65I–PstI subfragment from the mutant loricrin sequences was fused to the GFP sequence to create GFP(ML.VS Acc65I/PstI). Four potential NLS were amplified by PCR using GFP(ML.VS Acc651/PstI) as a template and fused to the GFP tag. After PCR amplification, the four PCR fragments were sequenced, digested with NheI and BamHI, and cloned into the pEGFPC-1 vector, resulting in plasmids GFP(NLS1), GFP(NLS2), GFP(NLS3), and GFP(NLS4). Oligo 3, 5′-GTGAACCGTCAGATCCGCTA-3′ was complementary to the 5′ end of the GFP tag in plasmid GFP(ML.VS Acc65I/PstI); Oligo 4, 5′-ATATATGGATCCCCGCCGCCTCCGGGTACCGTCGACAGAAT-3′ was specific for NLS1; Oligo 6, 5′-ATATATGGATCCCCGCCTCCGCCTCCGGGTACCGTCGACTGCAGAAT-3′ was specific for NLS3; Oligo 5, 5′-ATATATGGATCCCCTCCGCAGCCACCGCCGGGTACCGTCGACTGCAGAAT-3′ was specific for NLS2; Oligo 4, 5′-ATATATGGATCCCCTCCTCCGCAGCCACCGCCGCTGCCTCCGGAAGAGCCACCTC CGGGTACCGTCGACTGCAGAAT-3′ was specific for NLS4. The BamHI site used in the cloning procedure is underlined. The NheI site used is at position 592 of pE6 FPC1.

The constructs were transfected into HeLa cells using the LT1 polyamine reagent (Mirus; PanVera) according to the method recommended by the supplier. HeLa cells were grown at 37°C, 5% CO_2, in OPTI-MEM medium (GIBCO BRL) supplemented with 4% FBS, 100 U/ml penicillin G, and 0.1 mg/ml streptomycin sulfate.

Quantitation of Transgene Expression by RNase Protection Assay

RNA from neonatal epidermis was isolated using RNazol B (Tel-Test, Inc.), according to standard protocols. In brief, separated epidermis was frozen in liquid nitrogen, ground to a powder, and mixed with RNazol B. The resulting slurry was mixed with chloroform (10:1). Samples were centrifuged, the upper aqueous layer was removed, and RNA was precipitated with ethanol. RNA was then pelleted by centrifugation and resuspended in 50 μl of 1 μM EDTA. RNase protection assay (RPA) was performed using the RNase II kit (Ambion, Inc.), according to the supplied protocol. To accurately quantitate expression levels of the mutant loricrin transgenes relative to the expression of endogenous loricrin, a 375-nucleotide antisense probe was used for RPA that corresponded to the 3′ end of the mutant loricrin coding sequence. The 375-nucleotide probe was designed to be fully protected by the mutant loricrin transcripts, whereas wild-type transcripts would protect a sequence of only 350 nucleotides. RPA samples were run on a 6% acrylamide/8 M urea TBE gel followed by autoradiography and quantitation using a densitometer (Quick Scan Jr.; Helena Laboratories). All RPAs were performed using a glyceraldehyde 3-phosphate dehydrogenase (GAPDH) probe as an internal control for total RNA quantity.

Detecting a Barrier Dysfunction in Transgenic Mice

Transepidermal water loss (TEWL) from the ventral skins of neonatal mice was examined using a Tewameter TM210 (Courage and Khazaka), as described previously (Matsuki et al., 1998) (see Fig. 9 a).

We also used a simple dye penetration test to demonstrate barrier dysfunction in transgenic mice (Matsuki et al., 1998). The backs of neonatal mice were immersed in 1 mM Lucifer yellow in PBS (Fluka Chemical Co.). After 1 h of incubation, mice were killed, then frozen, and dorsoventrally sliced at a thickness of 5 μm. The sections were analyzed using fluorescence microscopy (see Fig. 9 b).

Results

Construction of the ML.VS Transgene and Generation of Transgenic Mice Expressing the VS Loricrin Mutation

To construct the ML.VS transgene, we inserted a cytosine residue at position 1190 of the loricrin coding sequence (1190insC). This point mutation results in a frameshift, which replaces the 86 COOH-terminal amino acids with missense amino acids (Fig. 1, schematic representation of vector construction and comparison of mutant and wild-type loricrin sequence). Furthermore, due to this frameshift mutation, the endogenous termination codon is not recognized, thereby extending the loricrin polypeptide by 22 amino acids.

10 ML.VS loricrin transgenic mice were identified by PCR analysis of their tail DNAs. Of these, three independently derived transgenic animals were bred separately to generate F1 offspring. All F1 mice that carried the transgene displayed similar phenotypic abnormalities that were inheritable, indicating that these aberrations could clearly be attributed to transgene expression rather than the transgene integration sites. One founder line, which contained three copies of the transgene, was selected for detailed analysis.

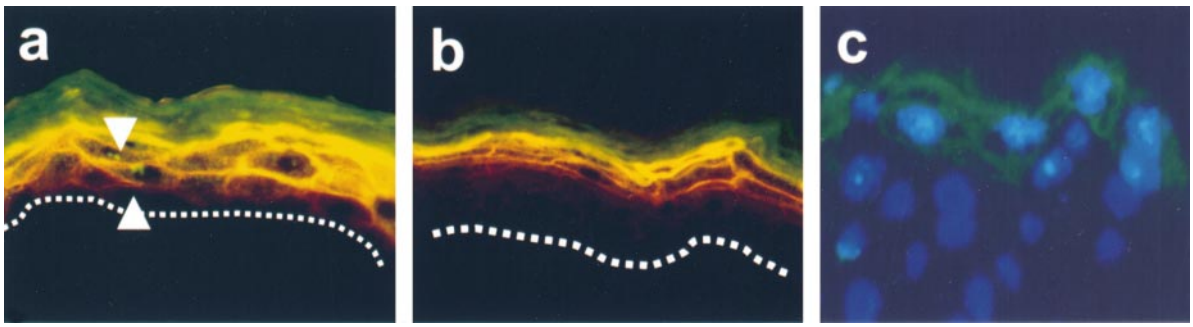

Figure 4. Immunofluorescence analysis to detect the VS mutant protein. (a and b) Double-immunofluorescent microscopy with LorNAb (FITC) and LorCAb (Texas red) antibodies. LorNAb detects expression of both endogenous and transgenic epitopes, whereas the LorCAb only detects endogenous epitopes. The LorNAb revealed a markedly strong and broad expression in ML.VS transgenics (a) compared with nontransgenics (b). The LorNAb (FITC) also detected immunoreactive granules within the nuclei in the suprabasal layers of ML.VS transgenics (a, arrowheads). Dots mark the dermo–epidermal interface. (c) Nuclear accumulation of the VS mutant protein is more apparent in ML.VS/Lor$^{-/-}$ neonatal skin (see below) stained with LorNAb and DAPI.

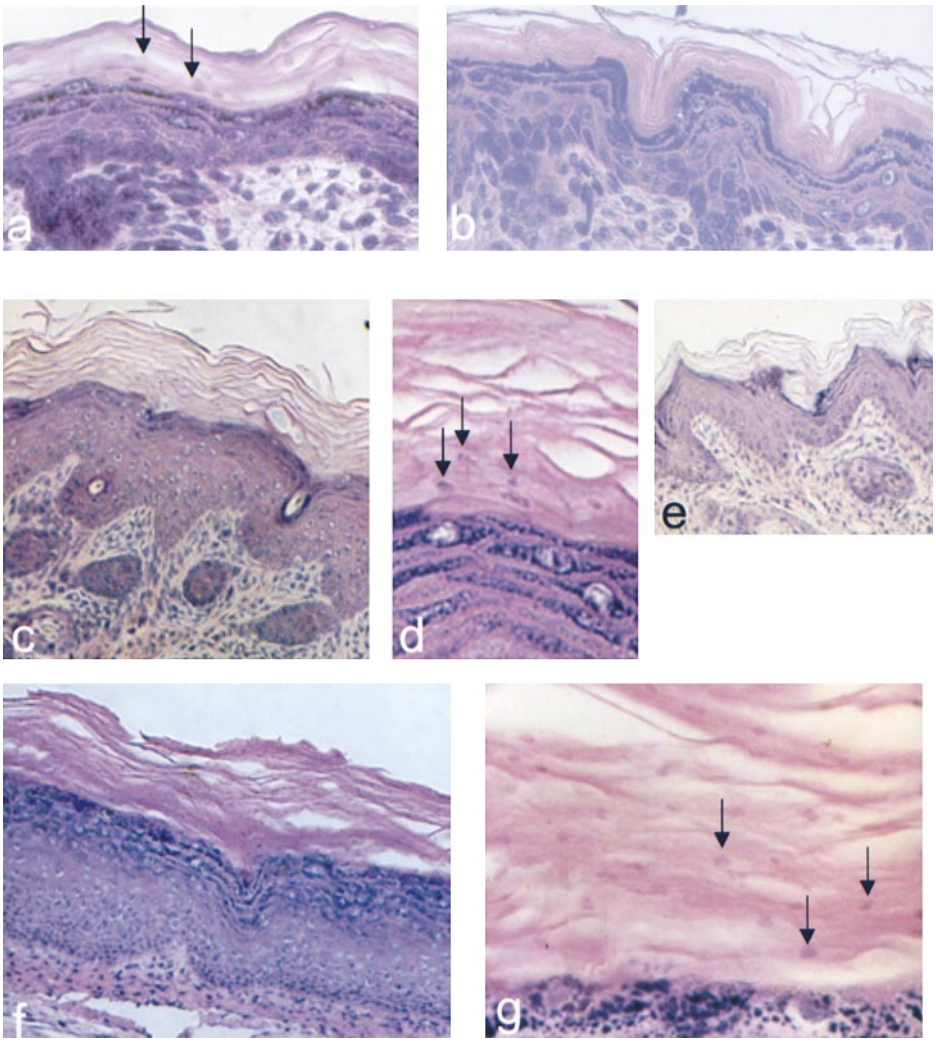

Figure 5. Histological analysis of ML.VS transgenic mice. Hematoxylin and eosin–stained paraffin sections of dorsal skin from transgenic (a) and nontransgenic mice (b). Note the remnants of nuclei present in the stratum corneum of transgenic skin (arrows). (c) Hyperkeratosis and parakeratosis were evident in the cornified cell layers around the constricting band in the transgenic tail. (d) Higher magnification of the cornified layers reveals the retention of nuclei (arrows). (e) Control tail. (f) Hyperkeratosis and parakeratosis were also evident in the transgenic footpad. (g) Higher magnification of f to demonstrate retention of nuclei (arrows).

All transgenic F1 pups from this founder had shiny skin when they were born, similar to that exhibited by the moderate F2 pup shown in Fig. 2 a (middle). They usually developed small scales over the whole body (ichthyosis) within the first 3 d of life (Fig. 2 b), which is consistent with ubiquitous epidermal expression of the loricrin transgene. The clinical appearance of this mouse phenotype is similar to that reported previously for a patient with VS associated with ichthyosis (Camisa and Rossana, 1984). However, the transgenic skin phenotype gradually disappeared and was absent in adult animals.

Since the human disease is inherited in an autosomal dominant fashion, we assume that the mutant and normal alleles are expressed at comparable levels. In an attempt to determine the phenotypic consequences of increasing the expression level of the mutant gene in the mouse model, we generated animals that were homozygous for the transgene in F2. Homozygous F2 pups exhibited severe neonatal erythrokeratoderma with red, shiny, and taut skin (Fig. 2 a, left).

To verify that phenotype severity correlated with the level of transgene expression, we isolated RNA from the epidermis of F2 neonates and performed RPA. The RPA probe was designed to detect both wild-type and transgene-derived (mutant) loricrin transcripts (see Materials and Methods). The transgene expression levels were increased approximately twofold in the severely affected F2 pups compared with moderate heterozygotes (Fig. 3). Thus, phenotype severity correlated with the expression levels of the transgene.

To examine the expression pattern of ML.VS loricrin in the epidermis of transgenic animals, we performed immunofluorescence microscopy using antibodies specific for epitopes located on either the NH_2 (LorNAb) or COOH (LorCAb) terminus (Fig. 4). Expression of both the transgene and wild-type loricrin was only detected with LorNAb, since the ML.VS protein does not have the epitope recognized by LorCAb. Interestingly, granules immunoreactive with LorNAb were frequently observed within the nuclei of suprabasal keratinocytes of ML.VS transgenics (Fig. 4, a and c). Since these granules were not stained with LorCAb, which detects the endogenous loricrin protein, this staining pattern appears to result from accumulation of the mutant form of loricrin in the nucleus (see below).

Severely affected homozygous transgenic mice also developed additional phenotypes ~5 d after birth: a thickening of the epidermis around the buttocks, the base of the tail, and in the footpads (see Figs. 2, c, e, and f). At around day 7, transgenic mice showed a constricting band at the base of the tail (Fig. 2 d), similar to that seen around the digits of VS

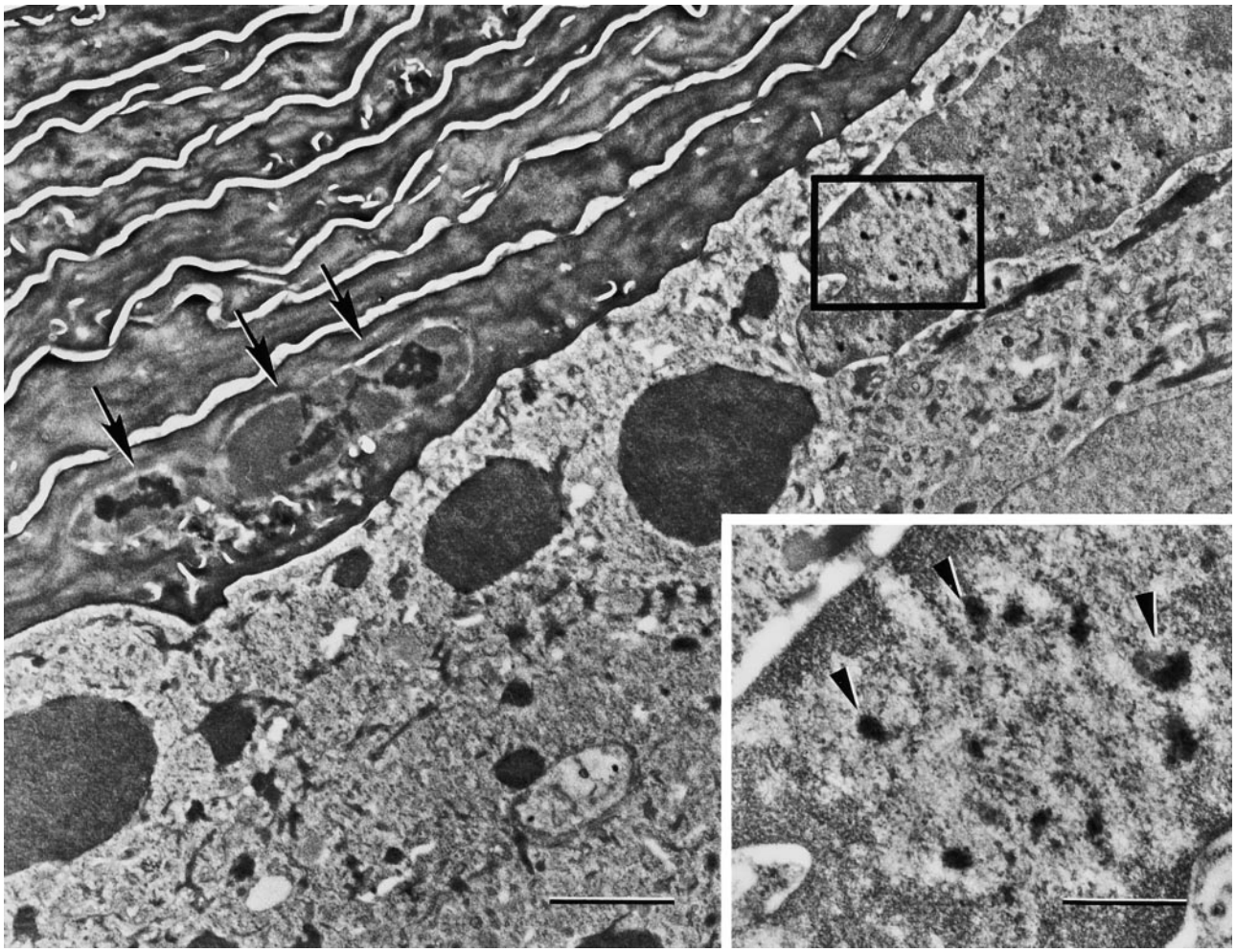

Figure 6. Ultrastructure of transgenic skin. Electron micrograph of a thin section through the upper epidermis from back skin of a transgenic ML.VS mouse. No gross morphological abnormalities in CE formation are evident in the transgenics, but parakeratotic nuclei are observed in the transitional layer (arrows). Moreover, in the nuclei of granular layer cells, electron-dense granules are visible (arrowheads, bottom right, in the enlargement of boxed area) that are not seen in normal siblings. Bars, 0.5 μm.

patients. The distal part of the constriction was usually slightly edematous because of the constriction. However, autoamputation, which is observed in VS patients, was not observed in homozygous pups and the phenotype became less severe and gradually disappeared after day 11 (data not shown). Similarly, hyperkeratosis of the footpads also became less evident after day 11 (data not shown). Although the ML.VS transgene was expressed in other tissues, such as tongue, esophagus, and forestomach, we were unable to detect an obvious phenotype in these tissues (data not shown).

Histopathology of ML.VS Transgenics

Histology of neonatal dorsal skin in homozygous transgenics showed parakeratosis, characterized by retention of nuclei in the stratum corneum (Fig. 5 a, arrowheads). Though the erythrokeratoderma phenotype suggested hyperkeratosis of the skin, thickening of the epidermis was not very pronounced in newborn transgenics. However, biopsies from the region of the constricted tail and footpads showed severe hyperkeratosis (Fig. 5, c and f). In addition, parakeratosis was much more evident in these biopsies (Fig. 5, d and g).

Figure 7. Immunoelectron microscopy of transgenic ML.VS mouse skin. Immunogold labeling was performed with LorNAb antibodies and 10-nm gold particles applied to sections of dorsal skin from biopsy samples, prepared according to the method of Tokuyasu (1980). Abnormal granular aggregates observed within parakeratotic corneocyte nuclei (a and b) and granulocyte nuclei (c) labeled positively with LorNAb. The aggregates have a somewhat different visual texture in these preparations compared with Epon embeddings (see Fig. 6). Note that these aggregates (arrows in a and c) do not colocalize with nucleoli. Nu, nucleus; No, nucleolus; Cy, cytoplasm. In contrast, with this antibody, normal skin shows diffuse cytoplasmic staining as well as staining of round L granules in the cytoplasm and nucleus (data not shown, see Steven et al., 1990; Jarnik et al., 1996). Positive labeling of the CE was observed for $Lor^{+/+}$ transgenics (a), but not for $Lor^{-/-}$ transgenics (c). These observations imply that for the former mice, the antibody is labeling wild-type loricrin in the cell envelope and the mutant loricrin in the intranuclear aggregates (see Results). In parakeratotic nuclei, we observe characteristic crescent-shaped features of low electron density (a and b, white arrowheads). Their origin is unclear but, to date, we have observed them only in parakeratotic nuclei and in Epon embeddings (data not shown) as well as in Tokuyasu preparations. Bar, 0.5 μm.

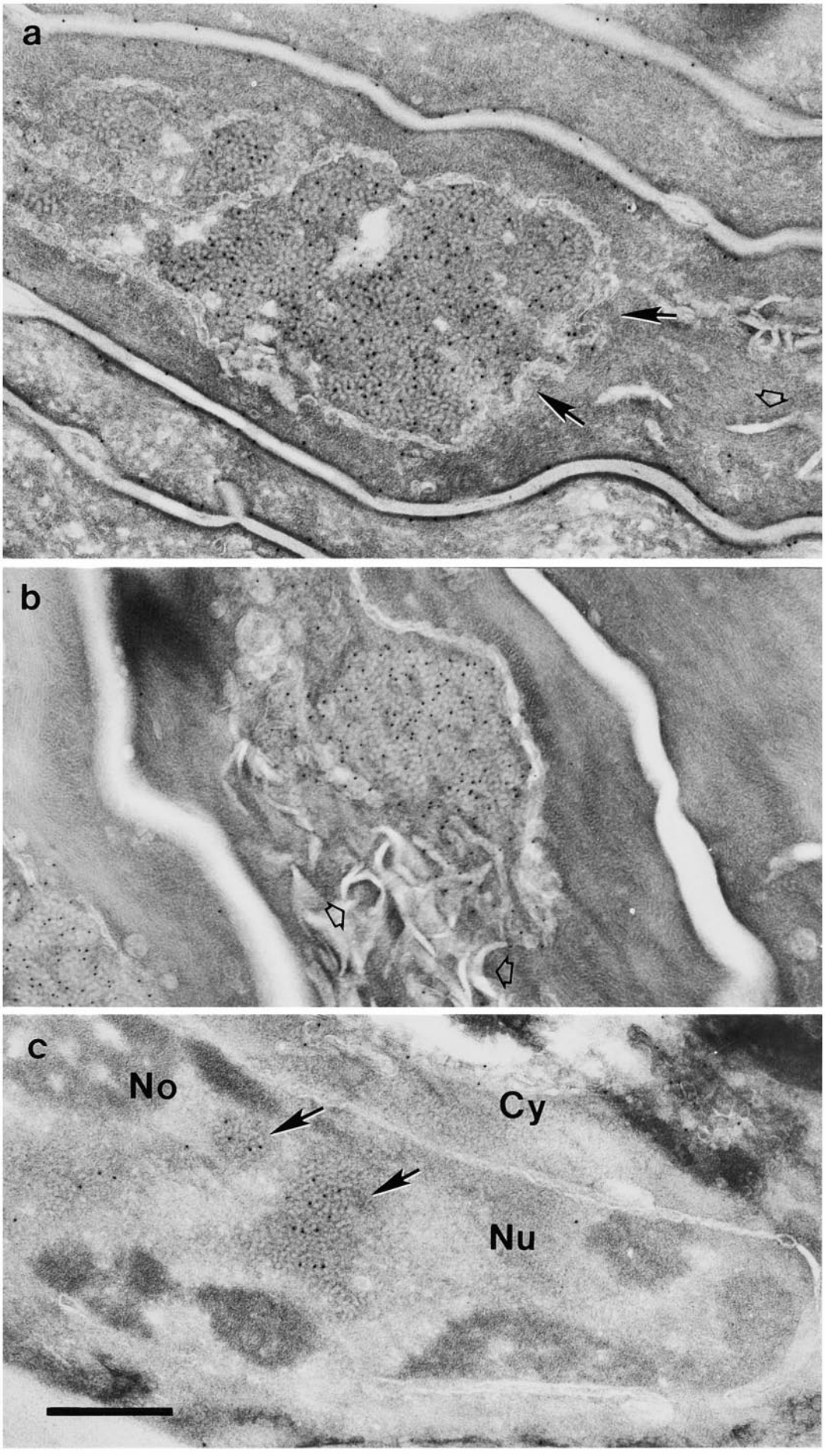

Figure 7.

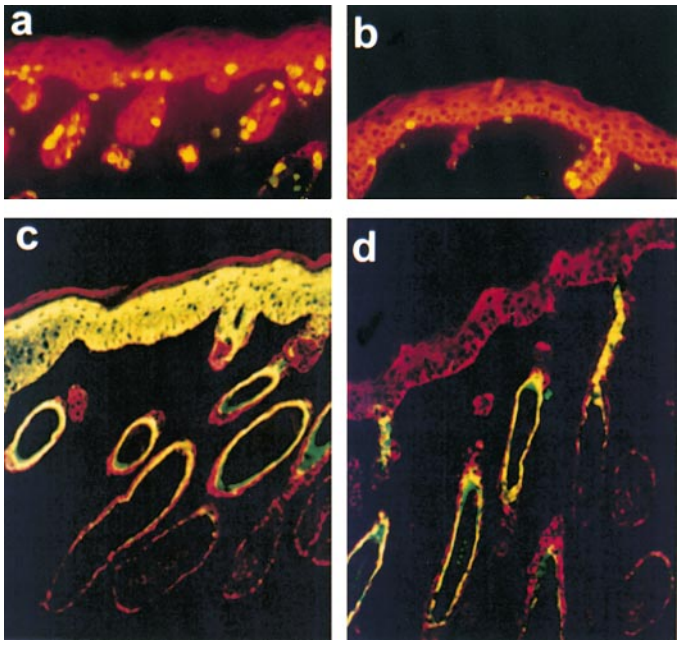

Figure 8. Increased BrdU labeling and interfollicular K6 expression in ML.VS transgenic epidermis. BrdU incorporation analysis was used to compare the distribution of S phase nuclei. BrdU labeling (yellow) of transgenic skin (a) shows an increase in mitotic activity versus control (b). Note the additional labeled nuclei in the basal layer in transgenic epidermis. The sections were also double-labeled with K14 (red). Marked interfollicular staining with an antibody to K6 (FITC) is evident in transgenic epidermis (c) compared with control (d). The epidermis was counterstained with antibody to K14 (Texas red). Yellow indicates colocalization at K14 and K6. In both cases, hair follicles stain positive for K6. Note strong interfollicular expression of K6 in transgenic tail from mice at day 7 after birth in addition to the staining of cells in the outer root sheaths.

At the light microscopy level, the only striking morphological abnormality in ML.VS transgenics was the parakeratosis in the cornified layers. Ultrastructurally, the granular, transitional, and cornified cell layers were slightly thicker than in normal epidermis, but keratohyalin granules appeared to be of the usual size and numbers. The most striking abnormalities were the presence of parakeratotic nuclei in the stratum corneum (Fig. 6, arrows) and of intranuclear condensates of moderate to high electron density in the upper granular cell layers (Fig. 6, arrowheads, bottom right). Immunoelectron microscopy showed that these condensates were recognized by LorNAb in both parakeratotic corneocyte nuclei (Figs. 7, a, arrows, and c) and granulocyte nuclei (Fig. 7 c, arrows). As expected, the CE labeled positively with LorNAb in ML.VS transgenic epidermis (Fig. 7 a) as well as in control epidermis (data not shown).

To assess potential changes in the proliferative compartment of phenotypic epidermis, control and severely affected newborn mice were labeled with BrdU for 1 h before killing. Staining with an anti-BrdU antibody showed an increase in mitotically active cells in transgenic epidermis (Fig. 8 a) over controls (Fig. 8 b). Transgenic epidermis had 60.5 ± 10.6 labeled nuclei/mm, whereas control epidermis had 32.2 ± 5.8 labeled nuclei/mm. The strong interfollicular induction of K6 in the acanthotic epidermis at the tail constriction (Fig. 8 c) and the epidermis of hyperkeratotic footpads (data not shown) was also consistent with hyperproliferation. As expected, K6 expression was restricted to the hair follicles in normal control littermates (Fig. 8 d).

ML.VS Mice Exhibit a Defect in Epidermal Barrier Function

The observation of dry, scaly skin suggested that ML.VS pups suffered from dehydration due to an epidermal barrier dysfunction. To examine this possibility, TEWL of ML.VS skin was assessed with an evapometer. TEWL was

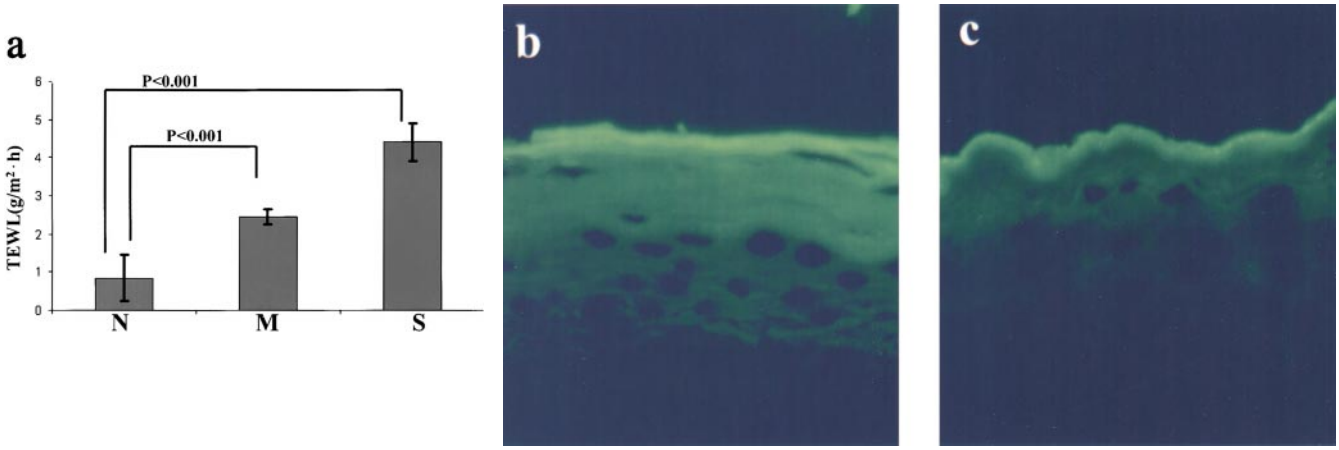

Figure 9. Defects in the skin barrier function of ML.VS transgenic mice. (a) TEWL was measured in transgenics and normal littermates. Note TEWL was increased more than fourfold in severely affected mice. Error bars represent SEM. Normal (N), $n = 20$; moderate (M), $n = 24$; severe (S), $n = 12$. (b and c) The fluorescent micrographs show the distribution of Lucifer yellow in the skin from severely affected (b) and control mice (c).

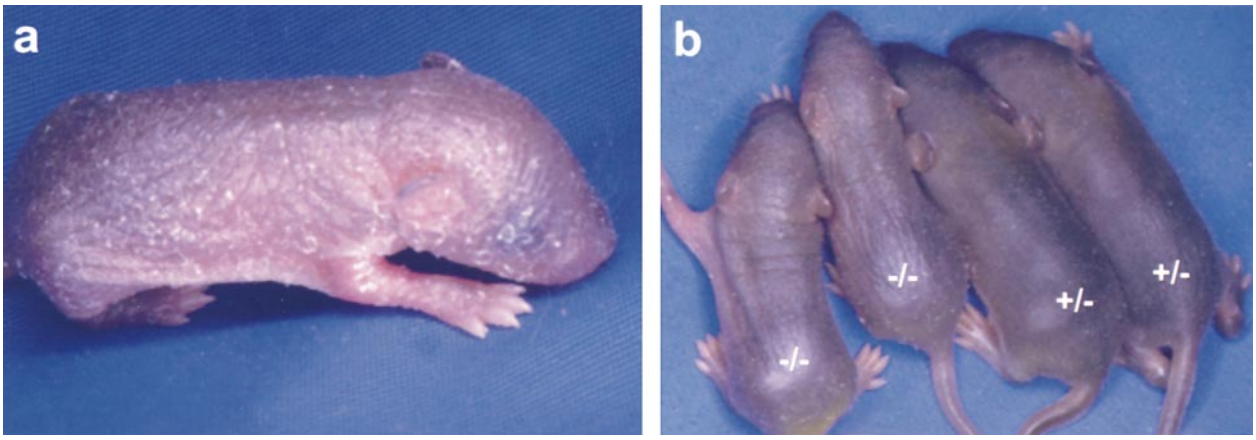

Figure 10. Macroscopic phenotype of ML.VS in the absence of endogenous loricrin (ML.VS Lor $^{-/-}$). (a) Newborn transgenics without endogenous loricrin expression seem to have a more scaly and dry skin phenotype than those with endogenous loricrin expression. (b) ML.VS transgenics that are heterozygous (ML.VS Lor$^{+/-}$) or homozygous (ML.VS Lor $^{-/-}$) for the loss of the loricrin gene at day 6. Note that the phenotype of ML.VS Lor $^{-/-}$ mice was more severe than that of ML.VS Lor$^{+/-}$ mice.

increased more than twofold and fourfold in moderately and severely affected transgenics, respectively (Fig. 9 a).

As an alternative method to evaluate epidermal barrier dysfunction, we examined the diffusion of the fluorescent dye Lucifer yellow through the epidermis (Matsuki et al., 1998). The dye was found to be retained in the upper layers of the stratum corneum in control neonatal mice (Fig. 9 c). In contrast, in severely affected transgenic pups, the dye penetrated significantly deeper into the epidermis (Fig. 9 b).

Introduction of the ML.VS Transgene into Loricrin Null Mice (ML.VS Lor$^{-/-}$)

To determine if the VS mutant protein was functioning in a classical dominant negative fashion, we bred the ML.VS transgenic mice with loricrin knockout mice (Koch et al., 2000, this issue). The severity of the ML.VS phenotype was slightly increased in transgenics that were heterozygous for the wild-type loricrin gene (Lor$^{+/-}$) compared with ML.VS transgenics that express both wild-type alleles (Lor$^{+/+}$), which was consistent with the mutant protein functioning as a dominant negative (data not shown). Unexpectedly, expression of the ML.VS transgene in the loricrin null background (Lor$^{-/-}$) showed a more severe phenotype than ML.VS mice in the Lor$^{+/-}$ background (Fig. 10 a), and as observed previously in the Lor$^{+/+}$ background, phenotype severity correlated with transgene dosage as evidenced via ML.VS/Lor$^{-/-}$ sibling matings (Fig. 10 b). Thus, these mating experiments confirm that the VS mutant protein is not functioning as a classical dominant-negative molecule, i.e., inducing the phenotype by a direct interference with wild-type loricrin.

Our initial attempts to examine the distribution of the VS mutant protein suggested that the VS protein accumulated in the nucleus; however, we could not determine whether the mutant was also present in the CE, since both the mutant and wild-type loricrin share the same NH_2-terminal epitope. The availability of ML.VS/Lor$^{-/-}$ mice allowed us to reexamine this question without this complication. Surprisingly, immunoelectron microscopy revealed that the VS mutant protein was almost exclusively present in the nucleus, with little if any incorporation in the CE (see Fig. 7 c). Thus, the positive labeling with the LorNAb seen on the cell envelopes of transgenics that also express wild-type loricrin (see Fig. 7 a, +/+ mice) presumably only detects the presence of wild-type loricrin.

The VS Form of Loricrin Contains Several Sequences That Meet the Criteria of NLS

A survey of the missense amino acids created by the frameshift mutation revealed several putative NLS (Dingwall and Laskey, 1991; Boulikas, 1993; Valdez et al., 1994) (Fig. 11 A). To determine whether these sequences were responsible for the nuclear accumulation of the VS form of loricrin, the following GFP fusion constructs were transfected into HeLa cells (Fig. 11 B). A vector with a BamHI–PstI fragment from wild-type loricrin (GFP[ML BamHI-PstI]) showed a homogenous protein distribution in the cytoplasm (Fig. 11 C, a). However, a vector with a BamHI–PstI fragment from the ML.VS transgene (GFP[ML.VS BamHI-PstI]) showed a patchy or granular distribution in the nuclei (Fig. 11 C, b). We also constructed a vector that contained the COOH-terminal missense amino acid sequence of ML.VS fused to GFP. The chimeric protein encoded by this vector also localized to the nuclei with a patchy or granular distribution (data not shown), suggesting that nuclear targeting resulted from sequences in the COOH terminus of the mutant loricrin protein. Four arginine-rich sequences within the COOH terminus of ML.VS were identified as possible NLS and tested in the GFP transfection assay. Only GFP(NLS4) showed a homogenous distribution inside the nuclei (Fig. 11 C, c). The other candidate sequences, GFP(NLS1–3), showed a cytoplasmic localization of the GFP fusion protein (data not shown). Thus, the bipartite NLS(NLS4) is responsible for the nuclear accumulation of the VS form of loricrin.

Discussion

To establish a causative relationship between loricrin mutations and the human skin diseases VS and PSEK, we introduced a transgene into the germline of mice containing a single nucleotide insertion that mimics frameshift muta-

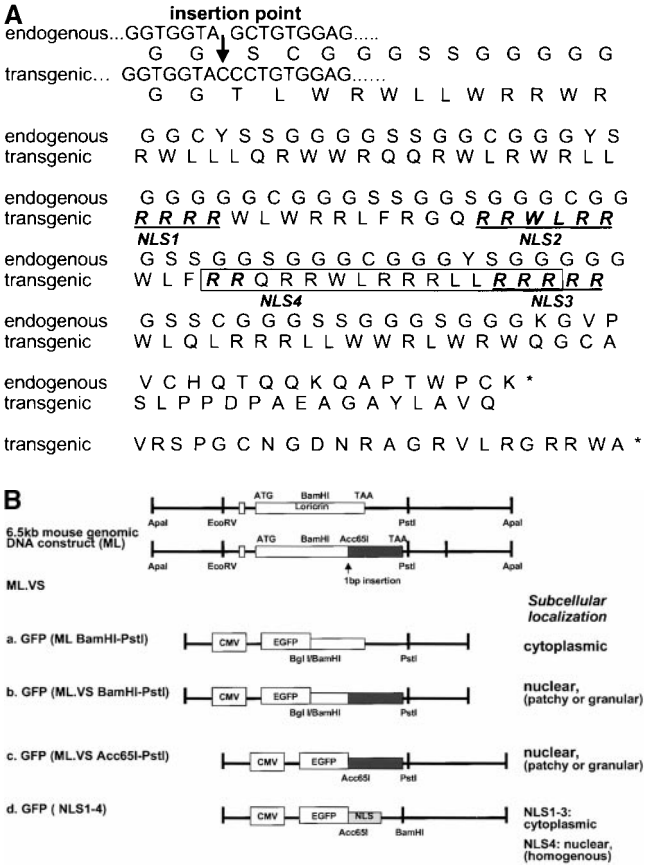

Figure 11. ML.VS loricrin sequence altered GFP localization in HeLa cells. (A) Comparison of wild-type and mutant COOH-terminal loricrin DNA and amino acid sequence resulting from a frameshift mutation and delayed termination of translation. The arrow points to the site of insertion of the point mutation in the ML.VS construct. Some motifs meeting the criteria of NLS in the mutant peptide are shown in bold type and underlined (NLS1–β3). The potential bipartite NLS is boxed, with the relevant basic residues in bold type (NLS4). (B) Diagram illustrating the subcloning of sequences from normal and mutant loricrin COOH terminus into the pEGFP-C vector. BamHI–PstI fragments from wild-type (a) and mutant loricrin constructs (b), respectively, Acc65I–PstI fragment (c), and four nuclear targeting motif candidates (d) from mutant loricrin were fused to the GFP protein. The mutant COOH terminus is represented by a black box. (C) Subcellular localization of GFP. GFP plasmids including the various sequences described above were transfected into HeLa cells. The subcellular localization of the expressed GFP was analyzed 24 h after transfection. GFP fluorescence was detected homogeneously in the cytoplasm of cells transfected with wild-type loricrin COOH terminus (a). However, fluorescence was detected in a patchy or granular pattern in the nuclei of cells transfected with mutant loricrin COOH terminus plasmid GFP(ML.VS.BamHI-PstI) (b) or GFP(ML.VS.Acc65I-PstI) (data not shown). GFP(NLS1), GFP(NLS2), and GFP(NLS3) constructs showed homogeneous distribution in the cytoplasm (data not shown). Only the NLS4 (bipartite NLS) construct was distributed homogeneously in the nuclei (c). Nuclei were visualized by staining with DAPI.

tions recently identified in VS and PSEK (Maestrini et al., 1996; Ishida-Yamamoto et al., 1997; Korge et al., 1997; Armstrong et al., 1998; Takahashi et al., 1999). Newborn mice expressing this mutant form of loricrin exhibited an erythematous and shiny skin**,** which immediately distinguished them from their nontransgenic littermates. This phenotype resembles the erythrokeratoderma observed in the human disease (Ishida-Yamamoto et al., 1997). Within the first 4 d after birth, the skin of transgenic neonates became dry and showed ichthyosis-like diffuse scales over the whole body. This phenotype is of particular interest since VS is a heterogeneous disease and a recent report suggests that loricrin mutations are only causative for VS associated with ichthyosis (Korge et al., 1997). Interestingly, the ichthyotic phenotype gradually disappeared in founder mice and their F1 progeny, in spite of unchanged expression of the transgene. We have also observed a gradual normalization of the congenital erythroderma phenotype exhibited by loricrin knockout mice (Koch et al., 2000, this issue). Taken together, these results suggest the existence of a compensatory mechanism that is induced in an attempt to restore epidermal barrier function.

Increased Expression of the Mutant Transgene Induces Additional Phenotypic Changes Similar to Those Observed in VS Patients

Since VS is transmitted in an autosomal dominant mode, we assume that both wild-type and mutant alleles are equally expressed. In an attempt to more closely mimic this expression pattern in the mouse model, we generated mice that were homozygous for the transgene in F2 and expressed essentially equivalent levels of mutant and wild-

type transcripts. At birth, homozygous ML.VS mice exhibited a severe erythrokeratoderma that resulted in a fourfold increase in TEWL compared with controls. The neonatal phenotype gradually progressed to a generalized ichthyosis, and with time, several additional phenotypic changes occurred that resembled clinical features of VS patients. Of particular interest was the formation of a constricting band at the base of the tail, similar to that seen around digits and toes of VS patients. Furthermore, the footpads developed nonepidermolytic hyperkeratosis.

The constricting band always formed at the base of the tail. Histologically, this area showed hyperkeratosis with parakeratosis and increased thickness of the epidermis. It is possible that this phenotype is due to a higher expression level of the transgene in the affected area. However, we did not find an increase in parakeratosis or LorNAb nuclear staining in sections from the base of the tail compared with the rest of the tail epidermis. It may be that the thickening of tail epidermis is due not only to expression of the mutant loricrin, but also to additional factors, such as mechanical stress, which might be particularly severe at the tail base. Although the digits of ML.VS mice never developed pseudoainhum, the footpads did exhibit nonepidermolytic palmoplantar keratoderma (NEPPK), which is another characteristic feature of VS patients. The molecular mechanism leading to NEPPK is unclear at present. However, the susceptibility of palms and soles might also be due to mechanical stress.

The Phenotype Induced by VS Mutant Loricrin Does Not Require a Direct Interaction with Wild-Type Loricrin

The availability of loricrin knockout mice provided us with the opportunity to determine whether the VS mutant was functioning as a classical dominant-negative molecule, i.e., was a direct interaction with wild-type loricrin required to induce the phenotype? It was already evident that the VS mutant was not simply inactivating wild-type loricrin; otherwise, the VS phenotype would have been identical to the loss of function phenotype observed in the germline deletion of the loricrin gene, i.e., a mild transient congenital erythroderma (Koch et al., 2000, this issue). Surprisingly, we found that the gain of function exhibited by the VS mutant did not require the presence of wild-type loricrin. In fact, the phenotype was exacerbated in the absence of loricrin. This suggests that the mechanisms compensating for the loss of loricrin (Koch et al., 2000, this issue) are impaired in their ability to maintain epidermal barrier function in the presence of the mutant form of loricrin. We also used tissue from ML.VS Lor$^{-/-}$ mice to determine the distribution of the VS mutant protein. Again to our surprise, immunoelecton microscopy demonstrated that the VS mutant form of loricrin was almost exclusively present in the nucleus, with little, if any, incorporation in the CE.

VS Mutant Loricrin Is Localized in the Nucleus and Not in the Cell Envelope

Although we cannot entirely exclude preferential masking of the NH_2-terminal epitope on VS mutant loricrin when cross-linked into the CE, this explanation appears unlikely since the antibody recognizes this epitope on wild-type loricrin in the CE and on mutant loricrin in intranuclear condensates. Moreover, our results are in agreement with previous observations in studies of the human diseases in which the same LorNAb was used to analyze clinical samples from both VS and PSEK patients. Immunoelectron microscopy revealed that intranuclear granules in the granular cells and nuclei in parakeratotic cornified cells were immunoreactive with the LorNAb, whereas the CEs in these samples were sparsely labeled (Maestrini et al., 1996; Ishida-Yamamoto et al., 1997). In retrospect, the latter labeling was probably of wild-type loricrin. Furthermore, to specifically determine the distribution of mutant loricrin in clinical samples, Ishida-Yamamoto et al. (Ishida-Yamamoto, A., H. Takahashi, and H. Izuka. 1999. *J. Invest. Dermatol.* 112:551 [Abstr.]) recently produced antibodies against a synthetic peptide corresponding to the sequences unique to the mutant loricrin. Consistent with the previous results, mutant loricrin was detected in the nuclei of differentiated epidermal cells and in parakeratotic nuclei of patient biopsies, but not in the CE.

Assuming that the residues used for cross-linking murine loricrin into the CE are distributed like those in human loricrin, which include Lys and Gln residues in the NH_2-terminal and internal non–Gly/Ser-rich domains (Steinert and Marekov, 1995), the question arises as to why the VS mutant loricrin, which is identical to wild-type loricrin in this part of the molecule, is not incorporated into the CE. Here the putative NLS in its COOH-terminal domain may provide an answer: it may lead to the mutant protein being transported efficiently into the nucleus, thereby preempting the formation of L granules in the cytoplasm or direct incorporation into the assembling CE. Such transport would also account for the large condensates of mutant loricrin that we observe in these nuclei.

How Does the Mutant Form of Loricrin Induce Phenotypic Changes in the Epidermis?

As discussed above, our mating experiments with the loricrin knockout mice establish that the phenotypes elicited by the mutant do not require the presence of wild-type loricrin. Furthermore, the immunoelectron microscopic data indicate that the mutant loricrin does not enter into the CE, but is mainly, if not exclusively, in the nucleus. Ultrastructurally, the CEs of ML.VS mice look normal. Since loricrin knockout mice assemble CEs of the usual thickness and uniformity, using other proteins as building blocks (Jarnik et al., manuscript submitted for publication), it appears likely that similar adaptations take place in the epidermis of ML.VS mice. Although it remains possible that the mutant loricrin may somehow interfere indirectly with CE assembly, there are no strong indications that this is the case because adequate CEs appear to be assembled in either a +/− or a −/− background. Thus, the VS-related phenotypes appear to result not from a defective CE, but from expression of the mutant loricrin, which then accumulates in the nucleus of cells in the granular layer.

This phenomenon may be responsible for disrupting the process whereby the nucleus is normally broken down during maturation of granular layer cells to corneocytes so that parakeratotic cells are found in the stratum corneum. The presence of parakeratotic cells may interrupt the orderly deposition of flattened squames and the cohesive-

ness of the stratum corneum. This simplistic mechanism could contribute both to the observed defect in permeability barrier and to the ichthyotic phenotype. However, it does not account for pseudoainhum in an evident way, suggesting that the late stages of epidermal differentiation are perturbed in a more global manner. In future studies, it may be possible to elucidate these mechanisms further by preventing nuclear accumulation of the VS mutant through selective alterations in the putative nuclear localization sequence in the substituted COOH terminus of the mutant loricrin.

We thank Sonja Wojcik and Meral Arin for comments on the manuscript.

This work was supported by a National Institutes of Health grant (AR40240) to D.R. Roop. Y. Suga was partially supported by The Naito Foundation (grant 94-453), Japan. P.J. Koch was supported by a George V. Evanoff Research Career Development Award from the Dermatology Foundation.

Submitted: 3 May 2000
Revised: 2 August 2000
Accepted: 2 August 2000

References

Armstrong, D.K.B., K.E. McKenna, and A.E. Hughes. 1998. A novel insertional mutation in loricrin in Vohwinkel's keratoderma. *J. Invest. Dermatol.* 111:702–704.

Boulikas, T. 1993. Nuclear localization signals (NLS). *Crit. Rev. Eukaryot. Gene Expr.* 3:193–227.

Camisa, C., and C. Rossana. 1984. Variant of keratoderma hereditaria mutilans (Vohwinkel's syndrome). Treatment with orally administered isotretinoin. *Arch. Dermatol*. 120:1323–1328.

Dingwall, C., and R.A. Laskey. 1991. Nuclear targeting sequence—a consensus? *Trends. Biochem. Sci*. 16:478–481.

DiSepio, D., A. Jones, M.A. Longley, D. Bundman, J.A. Rothnagel, and D.R. Roop. 1995. The proximal promoter of the mouse loricrin gene contains a functional AP-1 element and directs keratinocyte-specific but not differentiation-specific expression. *J. Biol. Chem*. 270:10792–10799.

Dominey, A.M., X.J. Wang, L.E. King, Jr., L.B. Nanney, T.A. Gagne, K. Sellheyer, D.S. Bundman, M.A. Longley, J.A. Rothnagel, D.A. Greenhalgh, and D.R. Roop. 1993. Targeted overexpression of transforming growth factor alpha in the epidermis of transgenic mice elicits hyperplasia, hyperkeratosis, and spontaneous, squamous papillomas. *Cell Growth Differ*. 4:1071–1082.

Gibbs, R.C., and S.B. Frank. 1996. Keratoderma hereditaria mutilans (Vohwinkel). *Arch. Dermatol*. 94:619–625.

Hohl, D., T. Mehrel, U. Lichti, M.L. Turner, D.R. Roop, and P.M. Steinert. 1991. Characterization of human loricrin. Structure and function of a new class of epidermal cell envelope proteins. *J. Biol. Chem*. 266:6626–6636.

Ishida-Yamamoto, A., D. Hohl, D.R. Roop, H. Iizuka, and R.A. Eady. 1993. Loricrin immunoreactivity in human skin: localization to specific granules (L-granules) in acrosyringia. *Arch. Dermatol. Res.* 285:491–498.

Ishida-Yamamoto, A., J.A. McGrath, H. Lam, H. Iizuka, R.A. Friedman, and A.M. Christiano. 1997. The molecular pathology of progressive symmetric erythrokeratoderma: a frameshift mutation in the loricrin gene and perturbations in the cornified cell envelope. *Am. J. Hum. Genet*. 61:581–589.

Jarnik, M., T. Kartasova, P.M. Steinert, U. Lichti, and A.C. Steven. 1996. Differential expression and cell envelope incorporation of small proline-rich protein 1 in different cornified epithelia. *J. Cell Sci*. 109:1381–1391.

Koch, P.J., P.A. de Viragh, E. Scharer, D. Bundman, M.A. Longley, J. Bickbach, Y Kawachi, Y. Suga, Z. Zhou. M. Huber, D. Hohl, T. Kartasova, M. Jarnik, A.C. Steven, and D.R. Roop. 2000. Lessons for loricrin-deficient mice: compensatory mechanisms maintaining skin barrier function in the absence of a major cornified envelope protein. *J. Cell Biol.* 151:389–400.

Korge, B.P., A. Ishida-Yamamoto, C. Punter, P.J. Dopping-Hepenstal, H. Iizuka, A. Stephenson, R.A. Eady, and C.S. Munro. 1997. Loricrin mutation in Vohwinkel's keratoderma is unique to the variant with ichthyosis. *J. Invest. Dermatol*. 109:604–610

Maestrini, E., A.P. Monaco, J.A. McGrath, A. Ishida-Yamamoto, C. Camisa, A. Hovnanian, D.E. Weeks, M. Lathrop, J. Uitto, and A.M. Christiano. 1996. A molecular defect in loricrin, the major component of the cornified cell envelope, underlies Vohwinkel's syndrome. *Nat. Genet*. 13:70–77.

Maestrini, E., B.P. Korge, J. Ocana-Sierra, E. Calzolari, S. Cambiaghi, P.M. Scudder, A. Hovnanian, A.P. Monaco, and C.S. Munro. 1999. A missense mutation in connexin26, D66H, causes mutilating keratoderma with sensorineural deafness (Vohwinkel's syndrome) in three unrelated families. *Hum. Mol. Genet*. 8:1237–1243.

Matsuki, M., F. Yamashita, A. Ishida-Yamamoto, K. Yamada, C. Kinoshita, S. Fushiki, E. Ueda, Y. Morishima, K. Tabata, H. Yasuno, M. Hashida, H. Iizuka, M. Ikawa, M. Okabe, G. Kondoh, T. Kinoshita, J. Takeda, and K. Yamanishi. 1998. Defective stratum corneum and early neonatal death in mice lacking the gene for transglutaminase 1 (keratinocyte transglutaminase). *Proc. Natl. Acad. Sci. USA*. 95:1044–1049.

Mehrel, T., D. Hohl, J.A. Rothnagel, M.A. Longley, D. Bundman, C. Cheng, U. Lichti, M.E. Bisher, A.C. Steven, P.M. Steinert, S.H. Yuspa, and D.R. Roop. 1990. Identification of a major keratinocyte cell envelope protein, loricrin. *Cell.* 61:1103–1112.

Roop, D.R. 1995. Defects in the barrier. *Science.* 267:474–475.

Roop, D.R., C.K. Cheng, L. Titterington, C.A. Meyers, J.R. Stanley, P.M. Steinert, and S.H. Yuspa. 1984. Synthetic peptides corresponding to keratin subunits elicit highly specific antibodies. *J. Biol. Chem*. 259:8037–8040.

Roop, D.R., H. Huitfeldt, A.E. Kilkenny, and S.H. Yuspa. 1987. Regulated expression of differentiation-associated keratins in cultured epidermal cells detected by monospecific antibodies to unique peptides of mouse epidermal keratins. *Differentiation.* 35:143–150.

Steinert, P.M., and L.N. Marekov. 1995. The proteins elafin, filaggrin, keratin intermediate filaments, loricrin, and small proline-rich proteins 1 and 2 are isodipeptide cross-linked components of the human epidermal cornified cell envelope. *J. Biol. Chem*. 270:17702–17711.

Steven, A.C., and P.M. Steinert. 1994. Protein composition of cornified cell envelopes of epidermal keratinocytes. *J. Cell. Sci.* 107:693–700.

Steven, A.C., M.E. Bisher, D.R. Roop, and P.M. Steinert. 1990. Biosynthetic pathways of filaggrin and loricrin—two major proteins expressed by terminally differentiated epidermal keratinocytes. *J. Struct. Biol*. 104:150–162.

Takahashi, H., A. Ishida-Yamamoto, A. Kishi, K. Ohara, and H. Iizuka. 1999. Loricrin gene mutation in a Japanese patient of Vohwinkel's syndrome. *J. Dermatol. Sci.* 19:44–47.

Tokuyasu, K.T. 1980. Immunochemistry on ultrathin frozen sections. *Histochem. J*. 12:381–403.

Valdez, B.C., L. Perlaky, D. Henning, Y. Saijo, P.K. Chan, and H. Busch. 1994. Identification of the nuclear and nucleolar localization signals of the protein p120. *J. Biol. Chem*. 269:23776–23783.

Vohwinkel, H. 1929. Keratoderma hereditaria mutilans. *Arch. Dermatol. Syphilol*. 158:354–364.